Relationship between the transfer properties of the coating and impedance spectroscopy in reinforced cement-based materials

A. Aït-Mokhtar · O. Poupard · P. Dumargue

Abstract This study highlights the relationships between some transfer properties of cement-based material, which coats reinforcing steel and its impedance response in High Frequency domain. Transfer properties are mainly represented by the coating thickness, its chloride diffusion coefficient and its porosity. The diffusion coefficient and the porosity are linked to the w/c ratio. Results have shown that the impedance spectroscopy is a pertinent non-destructive tool to characterize the cement-based materials coating. For reasons of long time consuming, tests were limited to coatings made of cement pastes with low thickness. It seems desirable to extend the study to concrete coatings that are more representatives of real structures. Indeed, the closed relationships highlighted by the results make this methodology possible to be implemented on the case of concrete structures in order to optimize the monitoring with a non-destructive way of the maintenance and the repairs of working concrete structures.

Introduction

The corrosion of reinforcing steel in cement-based materials is a worldwide problem. This phenomenon has high economic costs related to maintenance and repairs of concrete structures damaged by corrosion. According to a report of the Organization for Economic Cooperation and Development (OECD) [1], the reinforced concrete corrosion is the major cause of deterioration of buildings. In USA, costs generated by the corrosion of reinforced concrete were valued at 1 billion $ per year [2]. For a given structure, this corrosion is mainly caused by chloride penetration through the reinforced steel coating because this phenomenon concerns not only structures in marine environment, but also other structures, which could be affected by deicing salts [3].

Since the initiation of corrosion depends widely on the chloride concentration at the steel surface [4], it is clearly established that the transfer properties of the coating, such as diffusion coefficient and porosity, control the chlorides flux. These transfer properties characterize the porous structure of the coating [5–7].

In the objective of predicting the corrosion of reinforced concrete structures over aging process, various studies were performed by using the electrochemical impedance spectroscopy (EIS) as a non-destructive tool. The general aim was to monitor corrosion of reinforcing steel embedded in cement-based materials. This method, introduced in 1980's in reinforced concrete studies [8], allows determining the specimen response on a large frequency domain. Indeed, the EIS was used to study both:

– the low frequency domain (LF) of the impedance response to characterize the reinforcing steel behavior in relation to the corrosion [9–13],
– the high frequency domain (HF) to monitor the hydration process of cement-based materials [14–17].

A. Aït-Mokhtar (✉) · O. Poupard · P. Dumargue
LEPTAB, University of La Rochelle, Av. Michel Crépeau,
F-17042 La Rochelle cedex, France
e-mail: kmokhtar@univ-lr.fr

In addition, the HF arc can be related to the rebar surface adsorbed species such as Cl^- and OH^- in the case of chloride corrosion.

Correlating the microstructure parameters with a non-destructive test such as impedance spectroscopy would be of great interest in monitoring maintenance of structures and repairing in civil engineering field. However, there is a lack in literature works of focusing on the interaction between the transfer properties of reinforcing steel coating and the impedance response according to long-term durability tests.

Therefore, the present work deals with the electrical properties characterizing the microstructure of the cement-based material coating. The aim is to establish the connection between diffusion coefficient and porosity variations and that of the translation along the real axis of the impedance response in high frequency domain (10 Hz–1 MHz). The study is specially focused on the determination of the evolution of the real part in the impedance response and its relationships with the transfer properties of cement-based materials coating in relation with chloride diffusion through this coating.

Note that this study is a part of a program which general objective was the monitoring by non-destructive methods the durability of reinforced concrete in chloride environment [4]. The goal was to characterize in the same time by one type measurement either the response of the cementitious coating and that of the passivation condition of the reinforcing steel.

Background aspects

The principles of Alternating Current (AC) impedance spectroscopy are described in details elsewhere [18]. The impedance is a complex function, having both real and imaginary components. For a given system, the impedance is usually plotted in the Nyquist diagram, as imaginary part versus real part, providing a convenient tool for determining various electrical response behaviors of the system. The typical diagram for an electrochemical cell is presented in Fig. 1. The salient features highlighted by the spectrum are labeled as follows:

- the resistance R_0 is given by the high frequency limit of the diagram,
- the resistance R_1 and the capacitance C_1 are given by the diameter of the high frequency loop,
- the charge transfer resistance R_{CT} and the double layer capacitance, contributing to the surface electrode phenomena, are given by the low frequency limit.
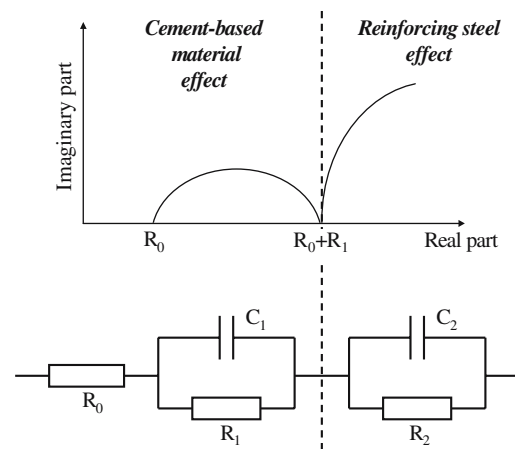

Fig. 1 Typical diagram of an electrochemical cell with its equivalent circuit model for impedance simulations

In case of systems associating cement-based material coating and reinforced steel, the high frequency loop (10 Hz–1 MHz), referred to the R_0, R_1 and C_1 parameters, seems to be linked to the microstructure of the coating.

Let R_{HF} be defined as the sum of the resistances R_0 and R_1.

Although this typical behavior is not accurately checked experimentally, researchers have agreed to describe the impedance spectra in three distinct features over a large frequency domain (1 mHz–1 MHz): high, intermediate and low frequencies [2, 18].

Equivalent circuits more complexes were proposed in literature to describe the combined system coating-reinforcing steel. However, the equivalent circuit, presented in Fig. 1, highlights the main behavior of this system.

Tests and Materials

Chlorides electrodiffusion tests

As the chloride diffusion coefficient is one of the parameters that describe the cementitious microstructure, electrodiffusion tests were performed to measure the diffusion coefficient of the cement-based material, which coats the reinforcing steel. A classical electrodiffusion cell was used (Fig. 2). A potentiostat applies a constant electrical field across the cement-based material specimen to accelerate the chloride transport. A four-point configuration was used: two platinum mesh and two reference electrodes, applied against the specimen faces to control the difference of potential imposed between these two faces. The downstream
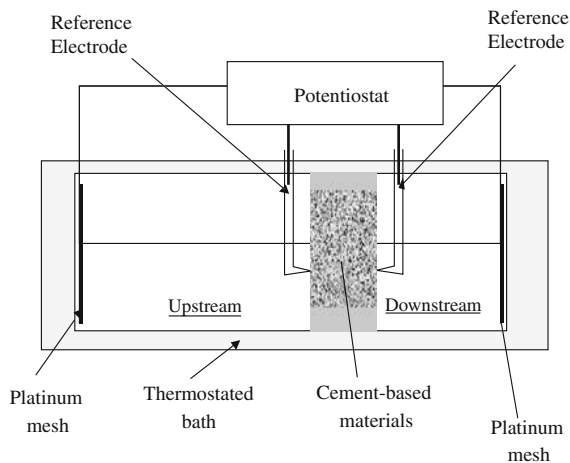
Fig. 2 Schematic view of the electrodiffusion cell

compartment contains a simulated pore solution (0.025 M NaOH and 0.083 M KOH). The upstream compartment is filled with a similar solution with an imposed chloride concentration (0.5 M NaCl). The experimental procedure was described in details by Aït-Mokhtar et al. [19]. Potentiometric titration tests with silver nitrate were performed in the downstream compartment after the NaCl addition. The measurement of the ionic flux in steady state allows deducing the diffusion coefficient from Eq. (1) [20]

$$D = \frac{RT}{z_{Cl^-} F} \frac{L}{U} \frac{\Delta C V_a}{\Delta t A C_0} \left(1 - e^{-\frac{RT}{zF}U}\right) \qquad (1)$$

where V_a (m³) is the downstream compartment volume; A (m²) is the cross-section area; ΔC (mol.m⁻³) is the variation of chloride concentration in the downstream compartment during a time range Δt (s); L (m) is the specimen's thickness; C_0 (0.5 M) is the chloride concentration in the upstream cell; R (J.mol⁻¹.K⁻¹) is the gas constant; T (K) is the reference temperature; Z_{Cl}^- the chloride ion valence; F (J.V⁻¹.mol⁻¹) is the Faraday constant and U (V) is the difference of potential applied between the two sides of the specimen.

Mercury Intrusion Porosimetry (MIP)

Mercury Intrusion Porosimetry (MIP) tests were performed by mercury injection measurements with a Micromeritics porosimeter, whose range of pressure reached more than 400 MPa. This pressure allows the mercury to penetrate pores of approximately 3 nm of diameter, according to Laplace's law.

Electrochemical Impedance Spectroscopy (EIS) measurements

Impedance spectra measurements were carried out by using a device composed by a Solartron potentiostat connected to a Frequency Response Analyzer (FRA) (Fig. 3). An alternating signal (DC field) of 20 mV is applied to ensure the linearity of the response. This value was checked experimentally [18]. The impedance measurements were performed at rest potentials. A three-point configuration was used: a counter electrode (large platinum mesh), a working electrode (reinforcing steel coated by a cement-based material) and a reference electrode (Saturated Calomel Electrode (SCE)). To cancel some artifact measurements in impedance response at high frequencies, a specific device was developed, which description is given in a previous work [21] (Fig. 3). The impedance data were recorded logarithmically down in the frequency range, from 1 MHz to 10 Hz.

Materials and conservation

Four types of coatings were manufactured: three types of cement pastes and a standard mortar (Table 1). The cement used was an ordinary Portland cement (OPC) of type of CEM-I 52.5 according to European standards EN 197–1. Its chemical composition is given in Table 2.

In addition, deionized water was used for the mixing in order to get a homogenous composition of the coating; i.e. without dissolved ions. The composition and preparation of the mortar comply with the European standards EN 196–1 (Table 1).

For all tests (electrodiffusion, MIP and EIS), the specimens manufactured had a prismatic form (100 × 100 × 200 mm³). Twenty-four hours after manufacturing, the specimens were demoulded and then cured during 28 days in an alkaline solution, which is identical to that of the tests. This solution simulates the pore solution of cement-based materials (0.083 M KOH and 0.025 M NaOH). This curing was carried out in order to ensure the specimens saturation and to reduce leaching phenomena.

For electrodiffusion tests, prisms of 100 mm side and 200 mm length were cast. After a same conservation than that of EIS specimens, core samples were taken from these prisms: disks of 75 mm diameter and 10 mm thickness. The external surfaces of these disks were covered with epoxy resin to limit the chloride transfer to one-dimensional direction (Fig. 3).
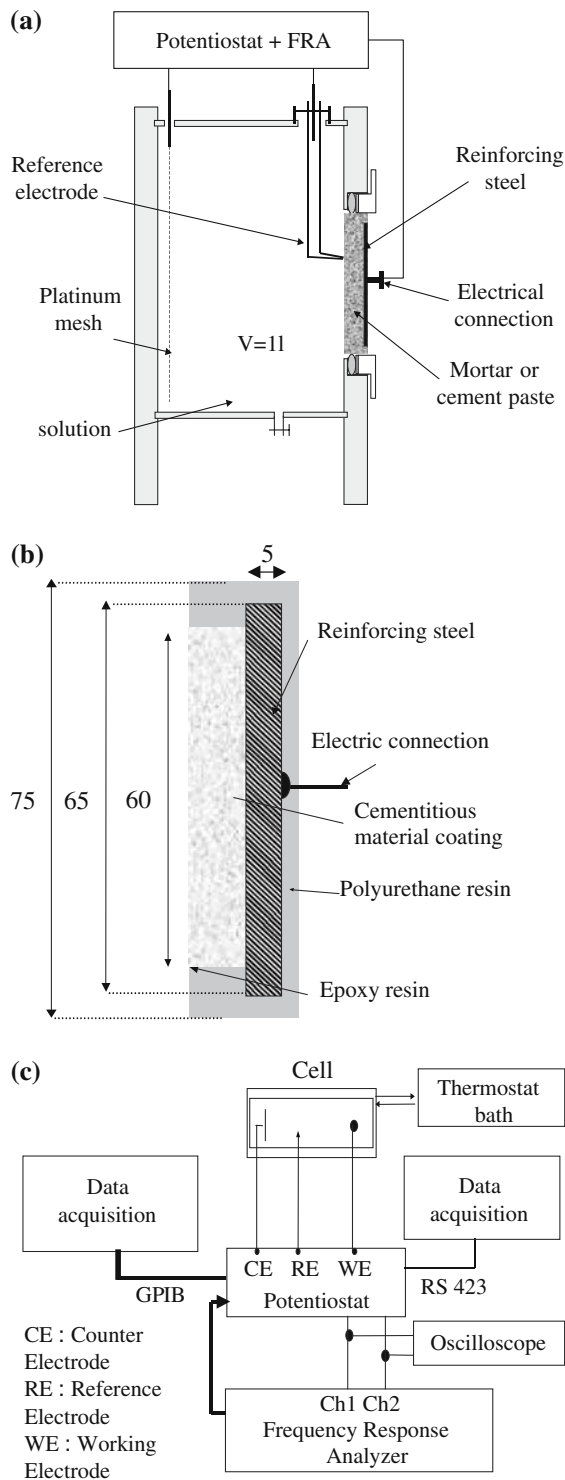
(a)

(b)

(c)

Fig. 3 Schematic view of (**a**) the electrochemical cell for EIS measurements (**b**) the sample (dimensions are in mm) and (**c**) the experimental device

For MIP measurements, samples were appropriated from the interior of the prisms described above and then dried during 24 h at 70 °C before tests.

Table 1 Composition of the cement-based materials coatings

Material	Designation	Water/ Cement (w/c)	Cement/ Sand (c/s)
Cement pastes	P0.3	0.3	–
	P0.5	0.5	–
	P0.7	0.7	–
Mortar	M0.5	0.5	0.33

For the EIS measurements, the cement-based material (paste or mortar) was cast on a circular reinforcing steel disc (60 mm-diameter, type: Fe E240). After being sand-blasted and rinsed with deionized water, the steel disc is covered on one face with the cement-based material whose composition and manufacturing are described above (Table 1).

To cancel wall effects, samples were obtained by a technique of core sampling on the initial prisms in order to have a cylindrical form with 65 mm diameter. The electrically connected face and the side faces of the cement-based material/reinforcing steel system were covered with a polyurethane resin to ensure a unidirectional chloride transfer (Fig. 3b). The required thickness is obtained by sawing and polishing the cement coating just before the EIS tests: from 10 to 1 mm for cement pastes samples and only 1 cm for the mortar ones. Coatings thickness was then measured accurately on nine points by using a sounding lead. Table 3 gives an overview of the samples characteristics.

Results: transfer properties

Diffusion coefficient measurements

Chloride titration allows getting the cumulated concentration in the downstream cell over time for the tested materials (Fig. 4). The diffusion coefficients are then calculated from Eq. (1) (see Table 4). Results obtained are in agreement with those given in literature [22]. In addition, they confirm that more the water/cement ratio is important; the more the diffusion coefficient is high.

Mercury intrusion porosimetry measurements

The pore size distributions for the samples tested are given in Fig. 5. Global porosities are obtained from these pore size distributions (Table 4).

Table 4 shows that the porosity obtained from MIP tests do not reflect the common values observed for these classical cement pastes according to Powers

Table 2 Chemical composition of the cement used

Oxides	CaO	SiO$_2$	Al$_2$O$_3$	Fe$_2$O$_3$	MgO	K$_2$O	Na$_2$O	SO$_3$	TiO$_2$	MnO	S$_r$O	P$_2$O$_5$
Composition (wt.%)	64.02	19.81	5.19	2.38	0.9	1.11	0.06	3.5	0.28	0.05	0.15	0.16

works [23]. Explanations can be done. As noticed in the literature [24], MIP tests do not investigate all pores in cement-based materials since a part of the porosity (micro-pores with size < 3 nm) is due to interstitial space in hydrated calcium silicates. This hydrate represents about 70% of the hydrated species in case of OPC. In addition, samples drying at 70 °C during 24 h before tests could be insufficient for the complete drying of the sample. However, this temperature was chosen in order to avoid disturbing of the microstructure arrangement of the sample before MIP test. Given these considerations, the porosity taken into account in the following discussions is that obtained from Powers model [23].

Table 3 Characteristic of cement-based material samples used in EIS measurements

Material	Sample no.	Average coating thickness (mm)	Standard value (mm)
P0.3	(1)	0.975	0.02
	(2)	1.060	0.02
	(3)	1.120	0.02
P0.5	(1)	0.600	0.02
	(2)	0.975	0.02
	(3)	1.090	0.05
	(4)	1.400	0.02
	(5)	10.0	–
P0.7	(1)	0.520	0.02
	(2)	0.650	0.10
	(3)	1.110	0.01
M0.5		10.0	–
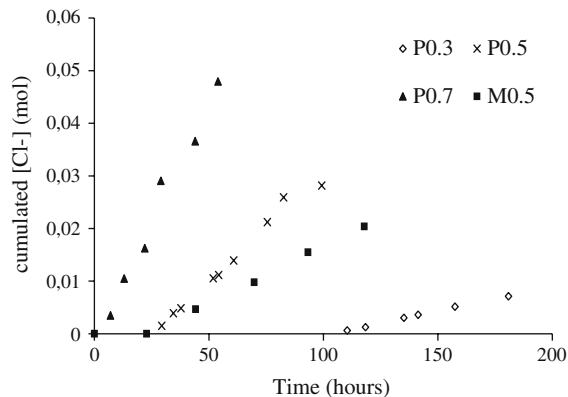
Fig. 4 Cumulative chloride concentration in the downstream of the electrodiffusion cell

Results and discussion: relationships EIS – microstructure properties

Comparison uncoated–coated reinforcing steel

Impedance measurements were carried out on uncoated and coated reinforcing steel. Results of the comparisons, plotted in the Nyquist diagram, are given in Figs. 6, 7. In these figures, the frequency decreases from left to right along the impedance curve. Figure 6 illustrates the influence of the w/c ratio and Fig. 7 shows the impedance response for cement paste and mortar. One can observe that

– for the uncoated steel immersed in the alkaline solution, only one loop with a large size describes the impedance response,
– for the samples having a thin thickness coating (about 1 mm), the impedance response has also one loop with a large size, but it has a translation along the Re-axis;
– the impedance response of the samples with a larger thickness coating (1 cm) is described by two well-distinguished loops: a small one in the HF domain and a larger one in the LF domain.

The diameter of the HF Arc (HFA) is obtained from the intersection between the low and high frequency curves with the real impedance axis, which corresponds to R_{HF}, as defined in Section 2. The comparison between the different cement pastes coatings; i.e. P0.3, P0.5 and P0.7; shows that this HFA diameter, i.e. R_{HF}, increases from 2 to 30 Ohms as the w/c ratio decreases (Fig. 6). This result agrees those suggested in literature [10, 12].

Some studies consider that the impedance response in the high frequency domain depends on the two phases of the cementitious material. These two phases

Table 4 Total porosity from MIP tests and from Powers, and diffusion coefficients of the tested samples

Material	Porosity MIP (%)	Porosity Powers (%)	Diffusion coefficient × 10^{-12} (m^2.s^{-1})
P0.3	17.76	14.5	1.36
P0.5	18.22	27.3	5.95
P0.7	27.90	47.3	13.40
M0.5	15.42	–	3.11

Fig. 5 Pore size distributions for the samples tested: (P) Cement pastes (M) Mortar
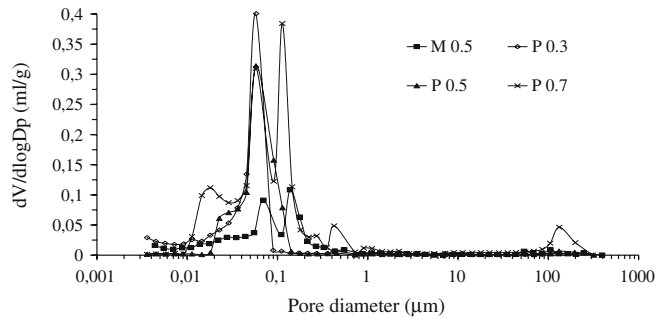
are the solid phase [25, 26] and the ionic mobility in the interstitial solution, which fills the pores of the material [27]. As the ionic conductivity of the interstitial solution can be considered constant, the variations of HFA diameter can be attributed to the reduction of the cross-sectional area induced by the coating. This reduction is linked to the porosity of the cementitious material: the section available for the ionic transfer increases in proportion with the porosity. This point is

Fig. 6 Impedance responses of naked steel and that coated by cement pastes (about 1 mm thickness)

Fig. 7 Impedance responses of naked steel and steel/cement-based material system (Mortar or Paste of 1 cm thickness)

highlighted below in the Section "Relationship EIS – w/c ratio and porosity".

Relationship EIS – Coating thickness

The thickness influences the HFA diameter (along the real axis R_{HF}). Figure 8 gives the impedance spectra for different thickness of cement paste coatings with w/c ratios of 0.3, 0.5 and 0.7, respectively. The figure shows a translation of the impedance response along the Re-axis versus the thickness of the coating: larger is the thickness; the more impedance response is shifted in the positive values of the real axis. Figure 9 depicts the variation of HFA diameter (along the real axis R_{HF}) versus the thickness of the three cement pastes.
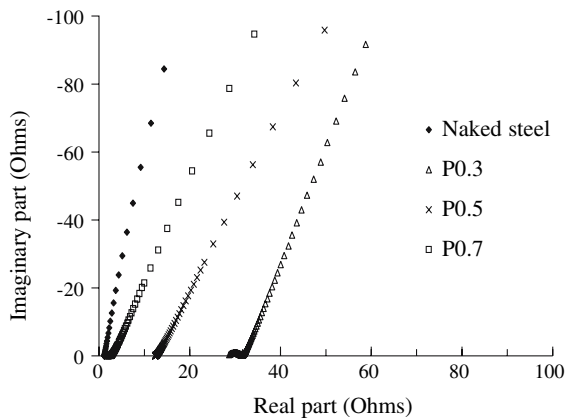
Comparison between Fig. 8a, and c shows that they give not the same evolution of real impedance translation according to the coating thickness. While these differences are not very significant in relative terms (relative evolution of R_{HF} versus relative evolution of the coating thickness), these differences mean that coating properties would be reflected on $R_o + R_{coating}$.

In addition, the type of evolution of R_{HF} versus the thickness coating is highlighted for the P0.5 sample coating in Fig. 10. This evolution seems to follow a logarithmic curve (Eq. 2) with a correlation coefficient of 0.988:
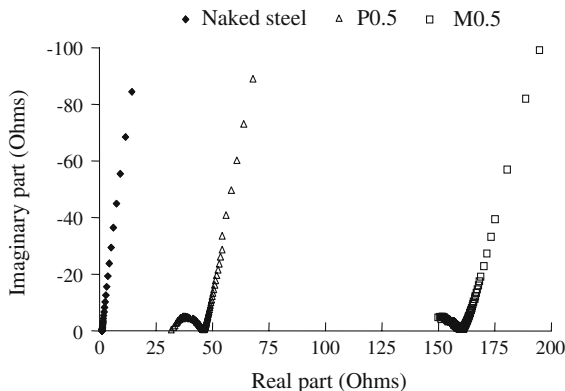
$$R_{HF} = 15.961n(e) + 10.36 \qquad (2)$$

where R_{HF} is expressed in (Ohms) and e is the coating thickness in (mm).

Relationship EIS – w/c ratio and porosity

Figure 8 highlights that the transfer properties of the cement-based material influence the impedance response in the HF domain. Note that the differences in the lower frequencies are due to some microscopic electrochemical phenomena that occur at the reinforcing steel surface.
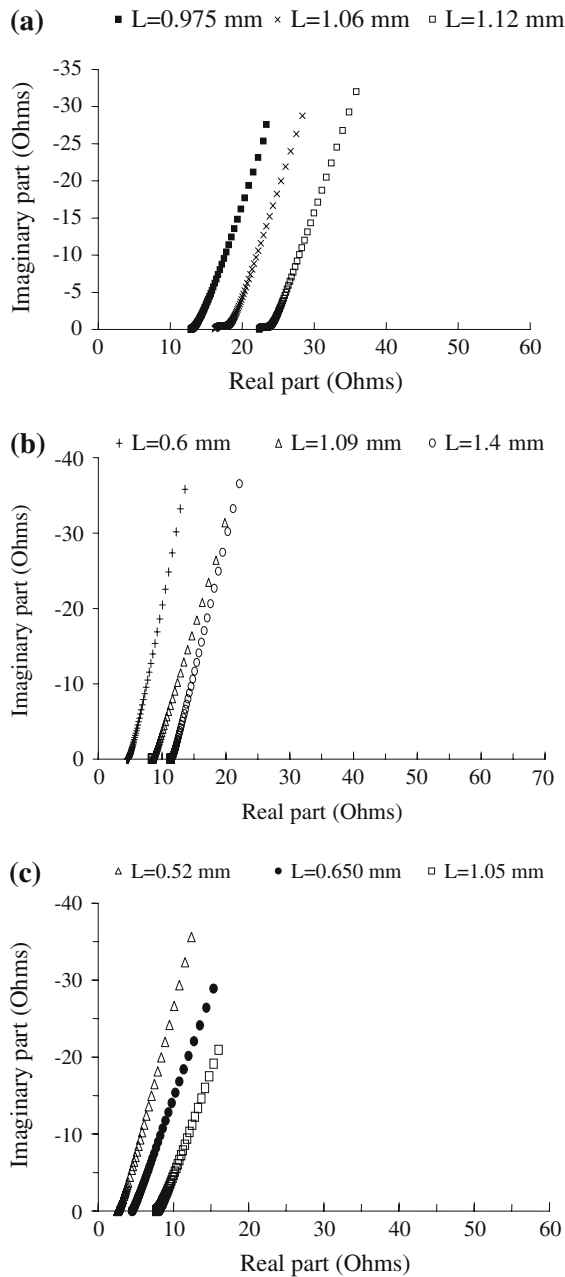
(a)

■ L=0.975 mm   × L=1.06 mm   □ L=1.12 mm

(b)

+ L=0.6 mm   △ L=1.09 mm   ○ L=1.4 mm

(c)

△ L=0.52 mm   ● L=0.650 mm   □ L=1.05 mm

Fig. 8 Impedance response versus thickness for cement pastes with different w/c ratios (a) 0.3 (b) 0.5 and (c) P0.7

Fig. 9 R_{HF} values versus the thickness of cement paste specimen (the thickness is noticed in the caption)

Fig. 10 R_{HF} evolution vs. thickness for w/c ratio = 0.5

adsorption that occurs between ions and the solid interface in the interstitial space of the material, known as electrical double layer and highlighted in chloride electrodiffusion in cementitious materials [19].

The variation of R_{HF} value in function of the w/c ratio of the material that embeds the reinforcing steel is given in Fig. 11. Figure 12 illustrates the relationship between R_{HF} value and the porosity of the cement pastes coating calculated from Powers model [23]. It is well known that the w/c ratio governs the materials porosity: the higher the w/c ratio, the higher is the porosity value. However, the comparison between Figs. 11 and 12 shows that this relationship is not linear. This would be due to the electro-capillary
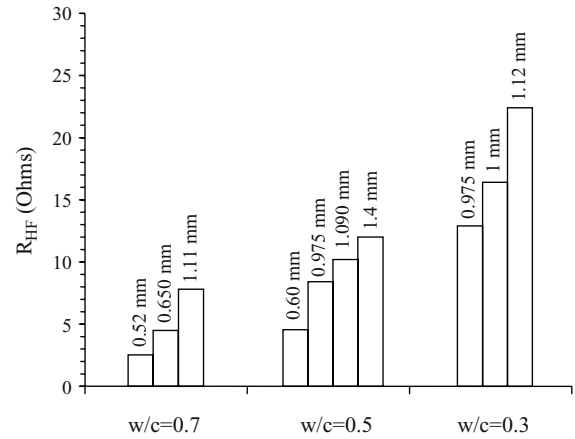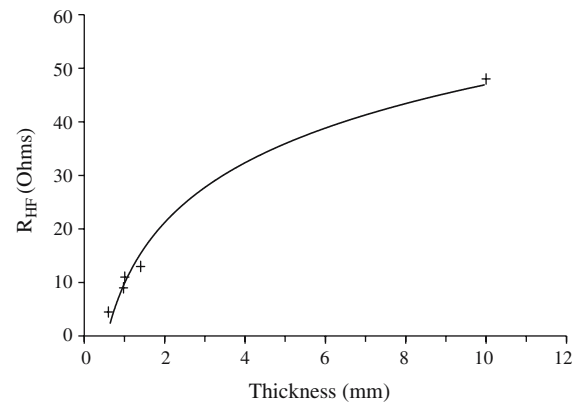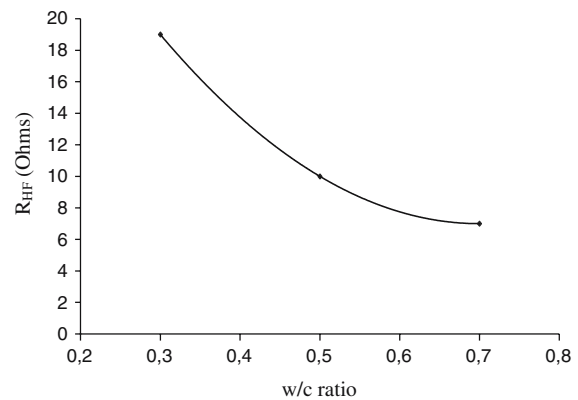

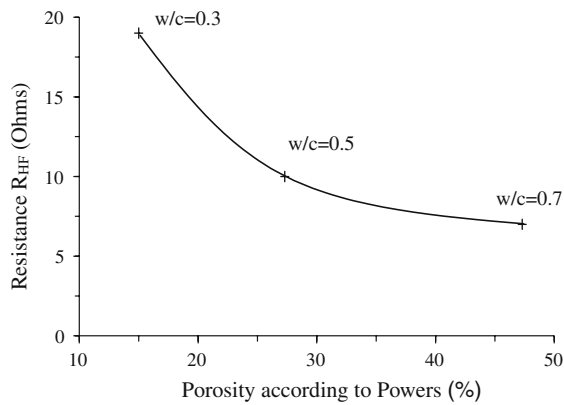**Fig. 11** Evolution of R_{HF} versus w/c ratio of cement pastes

Fig. 12 Evolution of R_{HF} versus porosity, according to Powers model [23]

Relationship EIS – Diffusion coefficient

In the same way as it was done for the porosity, Fig. 13 highlights the relationship between the diffusion coefficient of chloride and the impedance response in the high frequency domain.

One can observe that the evolution of R_{HF} versus the diffusion coefficient seems to be similar to its evolution versus the porosity given by Powers (Fig. 12). This can be explained by:

– on one hand, the Powers mode of calculation of porosity: the model takes into account all the water introduced in the cement paste, except the strictly necessary water for the cement hydration. Therefore, the obtained value of porosity is the maximum that the material can reach. In addition, the material's shrinkage is not taken into account in the calculation, whereas this later reduces the porosity,
– on the other hand, by the electrical double layer mentioned above, which the main effect is to slow
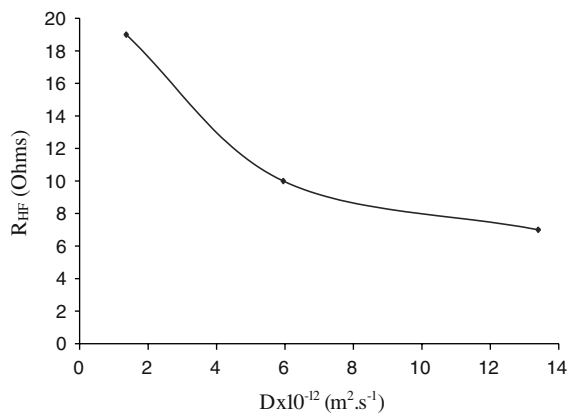

Fig. 13 Evolution of R_{HF} versus the diffusion coefficient

down the ionic transfer, particularly chloride ions on which the diffusion coefficient depends [19].

Conclusion

Although monitoring of the rebar corrosion activity by impedance spectroscopy is more important than the concrete coating monitoring, this paper highlights the close relationships between the AC impedance response in high frequency domain (translation of HFA along the real axis) and some transfer properties of cement-based material coating, in which reinforcing steel is embedded. These transfer properties concerns mainly the chloride diffusion coefficient and the porosity. In case of cement pastes, we have seen that both of these two parameters are directly linked to the water to cement ratio and express the microstructure properties of the material.

It remains that a longer time results and analyses is necessary for carrying out correctly this qualitative evaluation, and other techniques for the coating investigation remain necessary to get an accurate quantitative evaluation.

As a first approach, this study concerned only the case of cement pastes as coating. This case is not representative of the really structures in concrete. Therefore, it would be desirable to extend the study to concrete coating with the real thickness (some centimeters) even if our previous results [4, 21] have shown that the case of concrete would need a much longer laboratory experiments.

However, this extending to the concrete coating would be necessary to make the methodology presented in this work easier to be implemented in the case of concrete structures in aggressive environment. Going by these results, the objective is to carry out a non-destructive methodology for the monitoring of the coating and reinforcing steel conditions of working structures in the aim of planning the monitoring of diagnosis, maintenance and repairs.

References

1. Organization for Economic Cooperation and Development (OECD) (1989) According to a scientist expert group: durability of concrete bridges report, Paris (in french)
2. Ford SJ, Shane JD, Mason TO (1998) Cem Conc Res 28:1737
3. Tuutti K (1982) CBI Research report no 4.82. Swedish Cem. Conc. Res. Institute, Stockholm, Sweden
4. Poupard O, Ait-Mokhtar A, Dumargue P (2004) Cem Conc Res 34:991
5. Neville A (1995) Mater Struct 28:63

6. Ollivier JP, Marchand J, Nilsson LO (1996) In: Proceedings of the International RILEM workshop, Arles, France, September p 166

7. Lobet A (2003) in "Influence des paramètres de composition des matériaux cimentaires sur les propriétés de transfert", Ph.D. Thesis, INSA de Toulouse, France p 101 (in french)

8. John DJ, Searson PC, Dawson JL (1981) Br Corr J 16:102

9. Andrade C, Castelo V, Alonso C, Gonzalez JA (1986) In: Chaker V (ed) Corrosion effect of stray currents and the technique for evaluating corrosion of rebar in concrete (ASTM STP-906, Philadelphia, p 43

10. Gu P, Fu Y, Xie P, Beaudoin JJ (1994) Cem Conc Res 24:231

11. Hachani L, Fiaud C, Triki E (1994) Br Corr J 29:122

12. Andrade C, Keddam M, Novoa XR, Perez MC, Rangel CM, Takenouti H (2001) Elect Chem Acta 46:3905

13. Saremi M, Mahallati E (2002) Cem Conc Res 32:1915

14. Scuderi CA, Mason TO, Jennings HM (1991) J Mater Sci 26:349

15. Gu P, Xu Z, Xie P, Beaudoin JJ (1993) Cem Conc Res 23:531

16. Mccarter WJ (1996) J Mater Sci 31:6285

17. Christensen BJ, Coverdale RT, Olson RA, Ford SJ, Garboczi EJ, Jennings HM, Mason TO (1994) J Amer Ceram Soc 77:2789

18. Mcdonald JR (1987) In: Impedance spectroscopy: emphasizing solid materials and systems. John Wiley & Sons, New York

19. Ait-Mokhtar A, Amiri O, Poupard O, Dumargue P (2003) Cem Conc Comp 26:339

20. Amiri O, Ait-Mokhtar A, Dumargue P (2000) Rev Fr Gén Civ 4:161

21. Poupard O, Ait-Mokhtar A, Dumargue P (2003) J Mat Sci 38:2845

22. Tang L, Nilsson LO (1992) ACI Mat J 89:49

23. Powers TC, Brownyard TL (1947) J. Americ. Concr. Inst. 43 101, 249, 469, 549, 669, 845, 993

24. Ait-Mokhtar A, Amiri O, Dumargue P, Sammartino S (2002) Adv Cem Res 14:43

25. Keddam M, Takenouti H, Novoa XR, Andrade C, Alonso C (1997) Cem Conc Res 27:1191

26. Andrade C, Blanco VM, Collazo A, Keddam M, Novoa XR, Takenouti H (1991) Elect Chem Acta 44:4313

27. Cabeza M, Merino P, Miranda A, Novoa XR, Sanchez I (2002) Cem Conc Res 32:881